H$_2$S Gas Sensitivity of Doped SbP Monolayer：First Principle Study

Dong Li, Xiaolei Li*, Tengfei Wang, Lu Li and Junkai Wang

School of Materials Science and Engineering, Henan Polytechnic University,

Jiaozuo 454003, Henan, China.

lixl@hpu.edu.cn*

Summary: The sensing behaviors of monolayer antimonide phosphorus (SbP) for hydrogen sulfide (H$_2$S) are investigated by means of the density functional theory. In this paper, we calculated the best adsorption configuration, charge transfer, adsorption distance, band gap, electronic structure and recovery time of H$_2$S on the SbP monolayer and mental-doped SbP (X-SbP). The calculated results indicate that Al atom replaces Sb atom of SbP (Al-Sb-SbP), adsorption capacity was greatly increased, but the covalent bond formed between the gas molecules and the substrate was not suitable for sensing materials. And though Co or Ni atom could improve the interactions between H$_2$S gas and SbP sheets, the recovery time was too long. It was also not suitable for the sensor material of H$_2$S gas. However, for Pd doped SbP, Pd-Sb and Pd-P doping all exhibit excellent gas sensing performance for H$_2$S gas with the adsorption energy of -0.677eV and -0.520eV, the charge transfer 0.1113e and 0.0930e, the recovery time 0.19s and 5.30×10^{-4} s, respectively. These characters made Pd-SbP suitable for H$_2$S gas sensing material. Which further analysis we knew that these changes were mainly due to the orbital hybridization between the s, p orbitals of Pd atom and the p orbitals of S atom. Theoretical studies show that Pd-doped SbP is a promising H$_2$S gas sensing material.

Keywords: Monolayer SbP, Doped SbP, Density functional theory, Electronic structure, Gas sensors.

Introduction

Hydrogen sulfide (H$_2$S) is a kind of extremely flammable and a serious corrosive toxic gas, which is essential for real-time detecting of H$_2$S gas. [1, 2] Semiconductor gas sensors have high sensitivity, especially two-dimensional nanomaterials with large specific surface area and high carrier mobility [3]. By Comparing with traditional detection methods, the gas sensor based on new two-dimensional material had higher accuracy and sensitivity.[4, 5] Researchers have successfully developed sensors to detect small molecules of gases using graphene materials. [6] The detection of harmful gases by graphene sensor was studied by first principle study, and the optimal adsorption configuration and orientation of gas molecules on graphene surface was determined. [7] Although graphene had many excellent properties, it was a zero band gap semiconductor itself, which hinders applications as gas sensors. [8] In 2014, few layers of black phosphorus was successfully prepared, which had a direct band gap semiconductor with adjustable band gap value and high mobility. [9, 10] And black phosphorus had a puckered lattice structure, giving it a larger surface-to-volume ratio, which causes to a mass of adsorption sites. [11, 12] Compared the adsorption performance of black

phosphorene to different gases, black phosphorene sensor had strong selectivity to methanol gas, which might be used for methanol gas detection. [13] However, there were limited types of single phosphine adsorption gases. Formed by the combination of two elements for new material aroused considerable interests in application of gas sensors. [14] Monolayer SbP has been successfully predicted to have a fairly large band gap and high carrier mobility. [15] Black phosphorus Antimony had large surface area, which maximizes the factor of adsorbed gases on the sheet. In addition, monolayer antimonene probably had higher air stability than phosphorene and AsP [16] Guo et at. [17] demonstrated that monolayer SbP put up more significantly gas sensitivity to SO$_2$ than other gases. It could be applied to SO$_2$ sensor and SF$_6$ gas decomposition products detection.

It has been demonstrated that the adsorption capacity of doped 2D material to gas was significantly improved [18-21]. Fe-doped phosphorene and Fe-doped phosphorene with O$_2$ adsorption systems display potential dilute magnetic semiconductor and spin-polarized semiconducting properties respectively [22, 23]. Zhang *et al.*[24] studied the interaction of

---

doped-AsP with NO and H_2S molecules, and it was found that doping could significantly improve the sensitivity of AsP to H_2S molecules. For now, there is nearly no researcher of monolayer SbP as gas sensing applications. Also, there is no systematic study focused on doped-SbP based gas sensor for monitoring H_2S gas, so it is necessary to further study the adsorption characteristics of monolayer SbP to H_2S molecules.

Computational methods

In this study, the DFT program DMol[3] package [25] was used to carry out the interactions between H_2S molecules and SbP. The generalized gradient approximation (GGA) with Perdew-Burke-Ernzerhog (PBE) as the exchange-correlation potential was employed to research the electron-electron interaction [26]，and the double numerical polarization (DNP) basis set was chosen. In addition, due to the influence of the van der Waals (vdW)，the dispersion correted functional theory (DFT-D) with Grimme was made to amend. The energy and the force convergence tolerance were 1×10^{-5} eV and 0.002eV/ Å, respectively. A 3×3 supercell of monolayer SbP with a vacuum width of 20Å was adopted, which avoided interaction of the adjacent layers in the period structure. The K-point grid of 8×8×1 was set for both optimization and electric structure calculation to ensure high computational quality. The charge distributions between monolayer and H_2S molecule were analyzed on Hirshfeld method. During the all calculations, the H_2S molecule and the monolayer SbP were allowed to relax.

To characterize the adsorption strength of monolayer SbP or doped-SbP sheet for H_2S molecules adsorption, we computed the adsorption energy (E_a) by the following formula:

$$E_a=E_{SbP/\text{gas}}-E_{gas}-E_{SbP} \tag{1}$$

$$E_a=E_{doped\text{-}SbP/gas}-E_{gas}-E_{\ doped\text{-}SbP} \tag{2}$$

where $E_{SbP/gas}$、$E_{doped\text{-}SbP/gas}$、E_{gas}、E_{SbP} and $E_{\ doped\ SbP}$ are the total energy of H_2S gas adsorbed monolayer SbP system, H_2S/doped-SbP adsorption system, H_2S molecule, pure or doped SbP sheet, respectively. The more negative the E_a value, the more stable the adsorbed system.

The charge density difference (CDD) is defined as follows to intuitively observe the charge redistribution after H_2S molecules adsorption:

$$\Delta\rho=\rho_{SbP/gas}-（\rho_{SbP}+\rho_{gas}） \tag{3}$$

$$\Delta\rho=\rho_{doped\text{-}SbP/gas}-（\rho_{doped\text{-}SbP}+\rho_{gas}） \tag{4}$$

where $\rho_{SbP/gas}$、$\rho_{doped\text{-}SbP/gas}$、$\rho_{gas}$、$\rho_{doped\text{-}SbP}$ and ρ_{SbP} represent the electron density of monolayer SbP after H_2S gas adsorption, doped-SbP after H_2S gas adsorption, isolated H_2S molecule, pure or doped SbP sheet without H_2S gas adsorption.

The working principle of gas sensor is that the conductivity of the material will be changed when the gas is adsorbed on the surface of the material. The conductivity (σ) is obtained using the relation:

$$\sigma=A\ \exp(-Eg/2KT) \tag{5}$$

where C is constant, Eg is the band gap, T is the thermodynamic temperature(300K), and K is the Boltzmann constant (8.617×10^{-5}).

The sensitivity can be estimate via calculating the electrical conductivity of the pure or doped SbP sheet before and after adsorption were calculated by using the following relation:

$$S=(\sigma_{gas}-\sigma_{pure})/\ \sigma_{pure} \tag{6}$$

where σ_{gas} and σ_{pure} represent the electrical conductivity of the gas adsorption system and X-SbP itself, respectively.

In addition, another important parameter of gas sensor is recovery time, the speed of recovery time is the evaluation index of sensor reversibility:

$$\tau=V_0^{-1}\exp(-E_a/KT) \tag{7}$$

where V_0 is the attempt frequency, E_a is the adsorption energy, T is the thermodynamic, and K is the Boltzmann constant.

Results and Discussion

Model building

A stable substrate was first obtained before adsorbing H_2S molecules. The structure of the optimized monolayer SbP was shown in Fig. 1. (a). Firstly, we optimized the lattice parameters as flows: a=4.35Å and b=3.86 Å. The bond lengths of Sb-P in different directions were 2.62Å and 2.57Å, respectively, these parameters were basically consistent with previous reports [27]. The results above showed that the monolayer SbP structure was reliable.
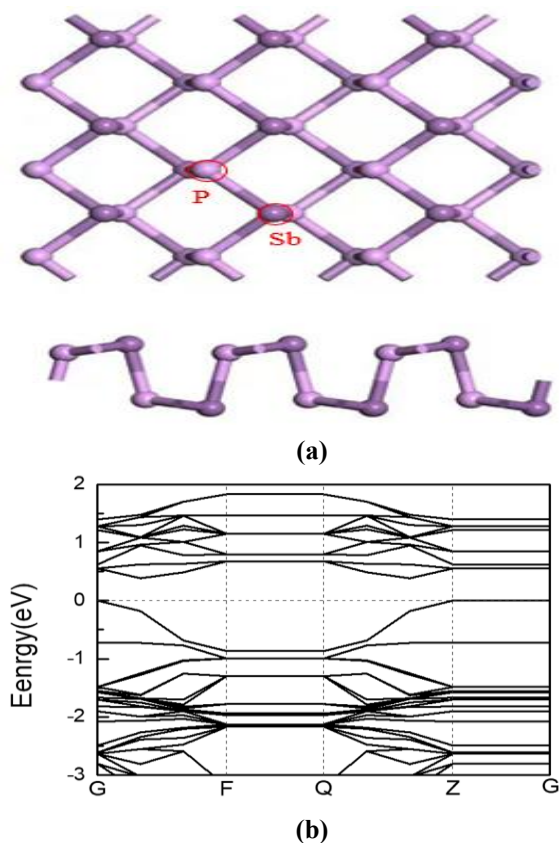
(a)

(b)

Fig. 1:   (a) The top and side views of pristine structure of monolayer SbP. (b) Band structure of monolayer SbP.

Adsorption of H₂S on pure SbP

For understanding the adsorption of monolayer toward H$_2$S gas, four adsorption positions were considered, namely, on top of the Sb atom (A), the center of Sb-P bond (B), top of the P (C), top of the irregular hexagon center (D). Furthermore, five adsorption orientations of H$_2$S molecules were chosen, including, S-H bond perpendicularly (a) or parallel (b) to monolayer SbP, three atoms in the same plane and parallel (c) to monolayer SbP, atom surface is "V" or "Inverted V" shape perpendicular to monolayer SbP, which were
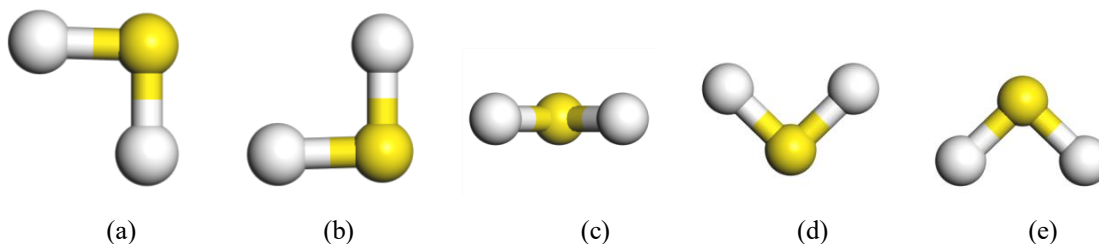
observed in Fig. 3. The most energetically favorable configurations were obtained by finding out the lowest-energy ones. The four adsorption positions adsorption energy (*E$_a$*), Hirshfeld charge (*ΔQ*), adsorption distance (*d*), recovery time(*τ*) and HOMO-LUMO band gap(*Eg*) of the lowest-energy H$_2$S molecules orientations, as listed in Table-1. For H$_2$S adsorbed on pristine SbP, the most negative adsorption is -0.289eV. The most favorable configuration was plotted in Fig. 2, the H$_2$S molecule tends to be adsorbed on the surface of SbP at an oblique angle, and S atoms of H$_2$S molecules were located above P atoms of monolayer SbP. Subsequently, we found the shortest distance between the atoms of SbP and H$_2$S molecule was 2.933 Å, which was much longer than H-P covalent bond (1.430Å [28]). Therefore, it could be preliminarily judged that the H$_2$S molecule was physisorbed on SbP via van der Waals interactions. Likewise, the charge transfer between H$_2$S molecule and SbP was only -0.0229e, which was confirmed the adsorption was weak physisorption. In addition, the HOMO-LUMO gap changes from 0.53eV of the monolayer SbP to 0.52eV, a change of 1.89%. The change of HOMO-LUMO gap was quite small, resulting in little change of conductivity of monolayer SbP after H$_2$S gas adsorption, which further indicates that intrinsic SbP was not suitable for H$_2$S gas sensor.
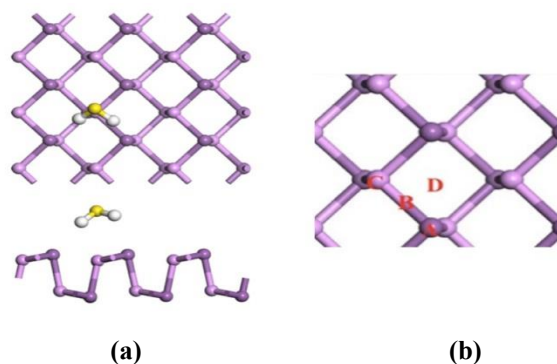

(a)   **(b)**

Fig. 2:   (a) The most stable configurations or H$_2$S adsorbed on monolayer SbP and (b) Four possible adsorption sites.

(a)   (b)   (c)   (d)   (e)

Fig. 3. Five orientation models of H$_2$S.

Table-1: Adsorption energy (E_a), Charge transfer(ΔQ), adsorption distance (d), recovery time (τ), HOMO-LUMO gap (Eg) of H_2S with different configurations on the monolayer SbP.

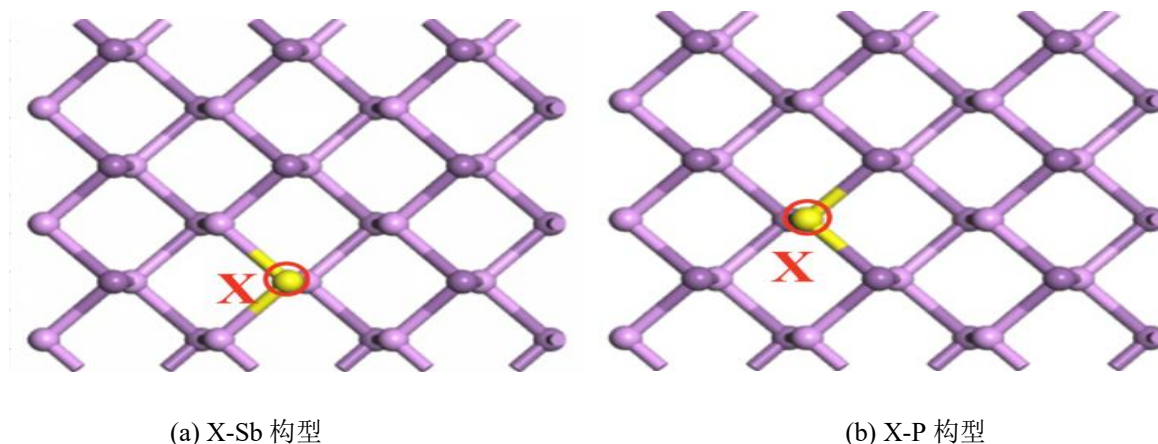| Adsorption site	E_a/eV	ΔQ/e	d/ Å	τ/s	E_g
A	-0.160	-0.0068	3.265	4.79×10^{-10}	0.52
B	-0.289	-0.0229	2.933	7.08×10^{-8}	0.52
C	-0.287	-0.0174	3.039	6.61×10^{-8}	0.52
D	-0.232	-0.0083	3.217	7.94×10^{-9}	0.52

(a) X-Sb 构型   (b) X-P 构型

Fig. 4: The Two doping structure for monolayer SbP: (a) X-Sb and (b) X-P；

Adsorption of H_2S on doped SbP

Based on the model of pure SbP, a doped SbP model was built by replacing the Sb atom or P atom with the X (X stands for Al, V, Co, Ni and Pd) atom. Two kinds of doping structure were observed in Fig. 4. The five orientations of H_2S molecules were consistent with those mentioned above, and the adsorption positions of H_2S gas were all located directly above the doped atoms. Consistent with the above, five adsorption orientations of H_2S molecule were considered, and the adsorption positions were all located directly above the doped atom. The calculated adsorption energy (E_a), Hirshfeld charge (ΔQ), adsorption distance (d), recovery time(τ) and HOMO-LUMO gap (Eg), were summarized in Table-2. It could be observed from Fig. 5 that the adsorption capacity of SbP doped with Sb atom was greater than doped with P atom. When the Sb atom of SbP was replaced by Al atom, it might be found the maximum negative adsorption energy and charge transfer are -1.096eV and -0.1894, which were obviously larger than the interaction of H_2S molecule on other metal atom doped SbP. T Nevertheless, it was found that the adsorption distance between the H_2S molecule and the substrate was 1.434 Å, which is similar to the theoretical length of H-P bond 1.430 Å. Combined with the above data, it could be inferred that the adsorption process was chemisorption processes. This means that the adsorption processes are irreversible. Nevertheless, it was found that the adsorption distance between the H_2S molecule and the substrate is 1.434 Å, which was similar to the

theoretical length of H-P bond 1.430 Å. For the Sb atom of SbP was replaced by Co or Ni atom, the adsorption distances were 2.301Å and 2.298Å, respectively, which were both larger than theoretical lengths of covalent bonds Co-S (2.14 Å) and Ni-S (2.13 Å). And the adsorption energies of two configurations are -0.897 eV and -0.843eV, respectively. In the other words, it was a physical adsorption of H_2S on Co or Ni doped SbP system. However, it was not suitable for sensing because the recovery time was too long. So we could infer that only for Co or Ni replaces P atoms of monolayer SbP, the substrate material could show excellent sensing properties of H_2S gas. While in the case of H_2S on Pd-SbP, no matter which atoms was replaced, the interaction between Pd-SbP and H_2S gas systems were enhanced. According to the data in the Table-2, when Pd atom was doped on SbP, the adsorption energy of Pd-Sb and Pd-P doping was -0.677eV and -0.520eV respectively, showing strong adsorption capacity; The recovery time was 0.19s and 5.30×10^{-4}s respectively, which was conducive to the reuse of the sensor; The band gap was 0.16eV and 0.18 eV, respectively; Before and after gas adsorption, the band gap changes 53.18 and 68.63%, respectively. Conductivity with band gap width change, the current will also produce a large change. From the observation of sensitivity Fig. 6, the sensitivity of Pd-SbP is relatively high upon the adsorption of H_2S gas. The conductivity changes greatly and the current changed obviously, revealing it was an excellent H_2S gas sensing material.

Table-2: Adsorption energy (E_a), Charge transfer (ΔQ), adsorption distance (d), recovery time(τ), HOMO-LUMO gap (E_g) of H$_2$S on X-doped SbP sheet.

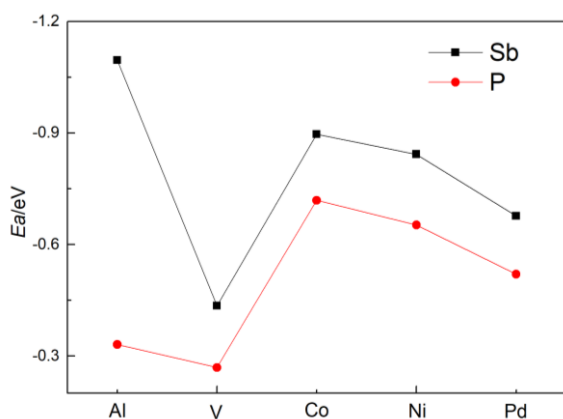| Doping site	E_a/eV	ΔQ/e	d/ Å	τ/s	E_g
Al-Sb	-1.096	-0.1894	1.434	2.58×10^6	0.53
Al-P	-0.331	0.0608	3.214	3.60×10^{-7}	0.28
V-Sb	-0.435	0.1540	2.597	2.01×10^{-5}	0.30
V-P	-0.269	0.1515	2.628	3.26×10^{-8}	0.19
Co-Sb	-0.897	0.1808	2.301	1.15×10^3	0.17
Co-P	-0.719	0.1501	2.292	1.20	0.26
Ni-Sb	-0.843	0.1012	2.298	143	0.19
Ni-P	-0.653	0.1618	2.304	0.09	0.19
Pd-Sb	-0.677	0.1113	2.552	0.19	0.16
Pd-P	-0.520	0.0930	2.569	5.30×10^{-4}	0.18

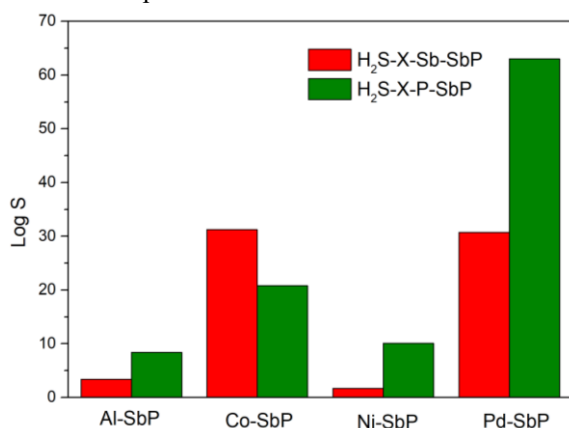Fig. 5: Adsorption energy of X (Al, V, Co, Ni, Pd) doped SbP.

Fig. 6: The sensitivity of different adsorbed system.

Electronic Structure of adsorbed H$_2$S with pure and Pd doped SbP

In order to more intuitively observe the charge redistribution between H$_2$S gas and the substrate, the charge density differential (CDD) of H$_2$S/ SbP, and H$_2$S/ Pd-SbP were plotted in Fig. 7. Clearly, there was almost no charge redistribution

between H$_2$S molecule and pure SbP substrate. While for H$_2$S/Pd-SbP system, it could be surveyed that the electrons were transferred from the surface of Pd-SbP to the H$_2$S, and the electrons were mostly accumulated on H$_2$S molecule. This discovery could be confirmed by analyzing the Mulliken charge, the substrate material is charge donor, in which the charge transfer of 0.1113 and 0.093eV were transferred from Pd-SbP monolayer to H2S molecule, respectively. The gain and loss of charge mainly occurred between H$_2$S molecule and substrate material, and the substrate material's sensitivity to H$_2$S molecule was greatly improved.

Meanwhile, to further verify the interaction mechanism between H$_2$S gas and SbP, the total density of states (DOS) and the projected density of states (PDOS) were displayed in Fig. 8. (Intercepted the DOS and PDOS near the Fermi level.) As shown in the figure, there was no significant change in the DOS of the pure SbP before and after H$_2$S adsorption, only had a little bit between -3eV and -2eV, where were far from the Fermi level. No obvious orbital hybridization was found in the PDOS diagram, which was consistent with the weak interaction between H$_2$S and pure SbP. As plotted in Fig. 8, different from the adsorption of H$_2$S on monolayer SbP, the adsorption of H$_2$S molecules could cause an obvious change in the DOS of Pd-doped SbP basal. For Pd atom replaced Sb atom of SbP, the p orbital of the S atom and the s and p orbitals of the doped Ti atom overlapped from approximately 1eV to 2eV. In addition, for Pd atom replaced P atom of SbP, we could also see that in the PDOS graph, similar orbital densities of s and p orbitals of Pd atom and p orbitals of S atom could be found from -0.5eV to 1.5eV, indicating the existence of slight orbital hybridization. The results of electron structure analysis suggested that orbital hybridization was the main reason for the increase of charge transfer and the enhanced interaction between H$_2$S molecule and Pd-doped SbP. Thus, Pd-doped SbP could be used as a potential H$_2$S gas sensor material.
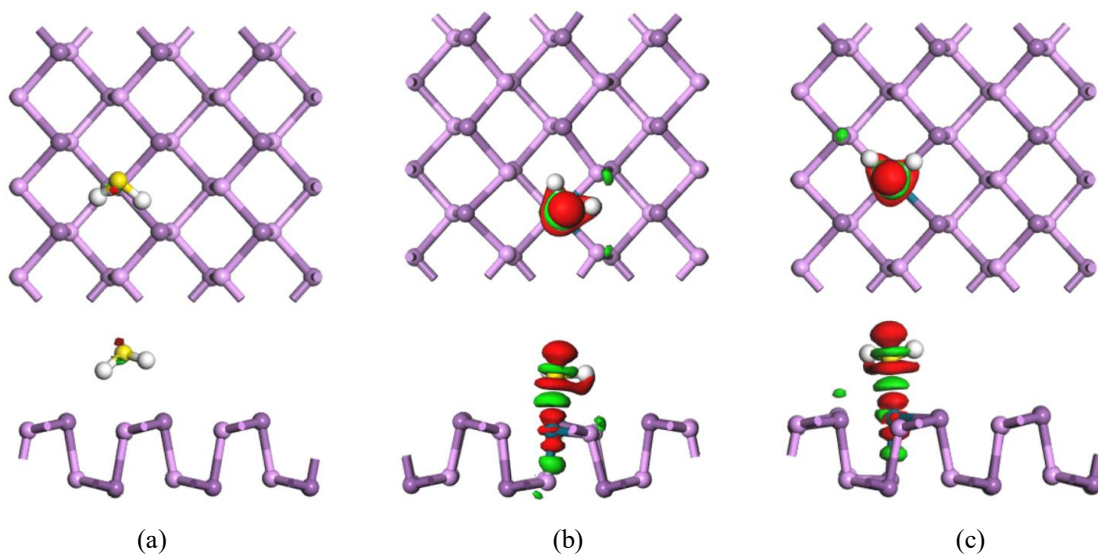
(a)　　　　　　　　　　　(b)　　　　　　　　　　　(c)

Fig. 7: The top and side views of the charge density difference for H_2S absorbed on (a) monolayer SbP (b) Pd -Sb-SbP and (c) Pd -Sb-SbP The isosurface value for all cases is 0.01e/ Å$^{3.}$
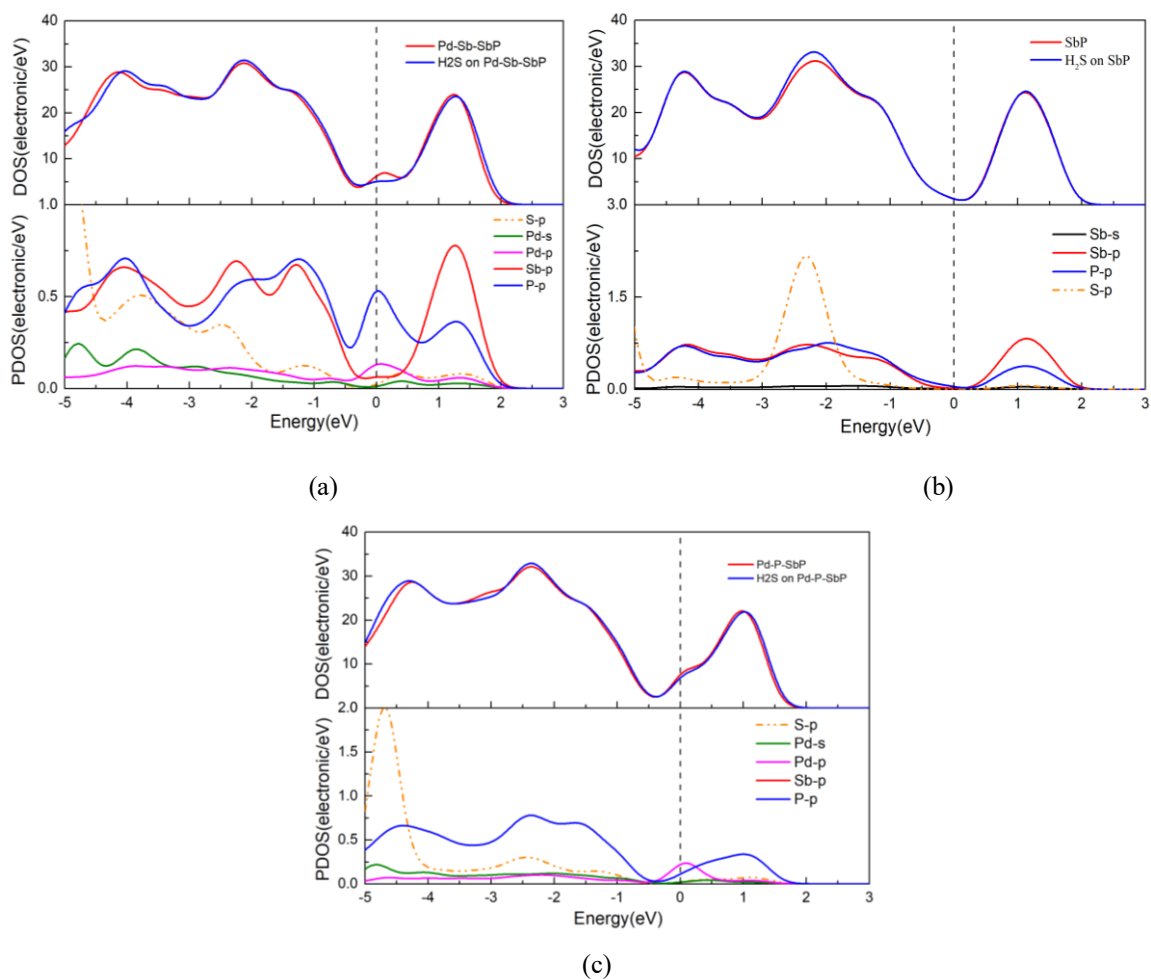

(a)　　　　　　　　　　　　　　　　　　　　(b)

(c)

Fig. 8: DOS and PDOS for different systems: (a)SbP and H_2S-SbP (b)Pd-Sb-SbP and H_2S-Pd-Sb-SbP (c)Pd-P-SbP and H_2S-Pd-P-SbP.

Conclusion

In this study, the first-principles calculations were carried out to explore the sensing properties of H_2S molecule onto pure or doped-SbP sheet. The results showed that the pristine SbP was insensitive to H_2S molecules, and the interaction force between H_2S and substrate materials was weak physical adsorption, which made it impossible to detect H_2S molecules effectively. The interaction force between Al-doped SbP and H_2S molecule was improved notably but the adsorption become chemical adsorption, which means that the adsorption process is irreversible. Though doping Co or Ni atom could improve the interactions between H_2S gas and SbP sheets, but the recovery time is too long, and it was also not suitable for the sensor material of H_2S gas. While for the Pd-doped SbP, the adsorption of H_2S onto Pd-SbP belonged strong physical adsorption. Meanwhile, according to the HOMO-LUMO gap analyzed that the resistivity of the materials would make a difference before and after H_2S adsorption on SbP sheet, which was beneficial to realize H_2S gas detection. Besides, short recovery time was conducive to the reuse of the gas sensor. Therefore, Pd-doped SbP can be a promising candidate material for H_2S gas sensors.

Acknowledgements

References

1. T. W. Lambert, Goodwin V. M., Stefani D., Strosher L., Hydrogen sulfide (H_2S) and sour gas effects on the eye. A historical perspective, *Sci.Total.Environ.*, **367**, 1 (2006).

2. O. Faye, Raj A., Mittal V., Beye A. C., H_2S adsorption on graphene in the presence of sulfur: A density functional theory study, *Comp.Mater.Sci.*, **117**, 10 (2016).

3. S. Manzeli, Ovchinnikov D., Pasquier D., Yazyev O. V., Kis A., 2D transition metal dichalcogenides, *Nat.Rev.Mater.*, **2**, 8 (2017).

4. C. Lee, Wei X., Kysar J. W., Hone J., Measurement of the elastic properties and intrinsic strength of monolayer graphene, *Science*, **321**, 5887 (2008).

5. J. S. Zavahir, Nolvachai Y., Marriott P. J., Molecular spectroscopy – Information rich detection for gas chromatography, *TrAC-Trend.Anal.Chem.*, **99**, (2018).

6. A. Geim, Novoselov K., Schedin F., Morozov S., Hill E., Detection of Individual Gas Molecules Absorbed on Graphene, *Nat.Mater.*, **6**, (2007).

7. Y. Peng, Li J., Ammonia adsorption on graphene and graphene oxide: a first-principles study, *Front.Env.Sci.Eng.*, **7**, 3 (2013).

8. W. Yuan, Shi G., Graphene-based gas sensors, *J.Mater.Chem.A.*, **1**, 35 (2013).

9. L. Li, Yu Y., Ye G. J., Ge Q., Ou X., Wu H., *et al.*, Black phosphorus field-effect transistors, *Nat.Nanotechnol.*, **9**, 5 (2014).

10. X. Ling, Wang H., Huang S., Xia F., Dresselhaus M. S., The renaissance of black phosphorus, *Proc.Natl.Acad.Sci (USA).* **112**, 15 (2015).

11. S. Y. Cho, Lee Y., Koh H. J., Jung H., Kim J. S., Yoo H. W., *et al.*, Superior Chemical Sensing Performance of Black Phosphorus: Comparison with MoS_2 and Graphene, *Adv.Mater.*, **28**, 32 (2016).

12. S. Lonkar, Singh K. K., Swaminathan S., Abdala] A., Recent advances in graphene based gas sensors, *Sensor.Actuat.B-Chem.*, (2015).

13. C. C. Mayorga-Martinez, Sofer Z., Pumera M., Layered Black Phosphorus as a Selective Vapor Sensor, *Angewandte Chemie*, **54**, 48 (2016).

14. S. Guo, Zhang Y., Ge Y., Zhang S., Zeng H., Zhang H., 2D V-V Binary Materials: Status and Challenges, *Adv.Mater.*, **31**, 39 (2019).

15. N. H. D. Khang, Ueda Y., Hai P. N., A conductive topological insulator with large spin Hall effect for ultralow power spin-orbit torque switching, *Nat.Mater.*, **17**, 9 (2018).

16. O. Üzengi Aktürk, Aktürk E., Ciraci S., Effects of adatoms and physisorbed molecules on the physical properties of antimonene, *Phys.Rev.B.*, **93**, 3 (2016).

17. H. Guo, Zheng K., Cui H., Zhang F., Yu J., Tao L.-Q., *et al.*, High sensitivity gas sensor to detect SF_6 decomposition components based on monolayer antimonide phosphorus, *Chem.Phys. Lett.*, **756**, (2020).

18. Z. M. A. A. B, B J. Y., B S. L., A Q. J., Enhancement of CO detection in Al doped graphene, *Chem.Phys.Lett.*, **461**, 4–6 (2008).

19. W. Wang, Zhang Y., Shen C., Chai Y., Adsorption of CO molecules on doped graphene: A first-principles study, *Aip Advances*, **6**, 2 (2016).

20. Y. L. Tian, Ren J. F., Yue W. W., Chen M. N., Hu

G. C., Yuan X. B., Adsorption of chloroform on N-doped and Al-doped graphene: A first-principle study, *Chem.Phys.Lett.*, **685**, (2017).

21. H.-p. Zhang, Luo X.-g., Lin X.-y., Lu X., Leng Y., Song H.-t., Density functional theory calculations on the adsorption of formaldehyde and other harmful gases on pure, Ti-doped, or N-doped graphene sheets, *Appl.Surf.Sci.*, **283**, (2013).

22. T. Hu, Hong J., First-Principles Study of Metal Adatom Adsorption on Black Phosphorene, *J.Phys.Chem.C.*, **119**, 15 (2015).

23. Y. Luo, Ren C., Wang S., Li S., Zhang P., Yu J., *et al.*, Adsorption of Transition Metals on Black Phosphorene: a First-Principles Study, *Nanoscale.Res.Lett.*, **13**, 1 (2018).

24. Y. Zhang, Tan C., Yang Q., Ye H., Chen X.-P., Arsenic Phosphorus Monolayer: A Promising Candidate for H2S Sensor and NO Degradation With High Sensitivity and Selectivity, *IEEE.Electr.Device.L.*, **38**, 9 (2017).

25. S. Grimme, Antony J., Ehrlich S., Krieg H., A consistent and accurate ab initio parametrization of density functional dispersion correction (DFT-D) for the 94 elements H-Pu, *J.Chem.Phys.*, **132**, 15 (2010).

26. N. Mardirossian, Head-Gordon M., omegaB97X-V: a 10-parameter, range-separated hybrid, generalized gradient approximation density functional with nonlocal correlation, designed by a survival-of-the-fittest strategy, *Chem.Phys.*, **16**, 21 (2014).

27. B. Cai, Xie M., Zhang S., Huang C., Kan E., Chen X., *et al.*, A promising two-dimensional channel material: monolayer antimonide phosphorus, *Sci.China.Mater.*, **59**, 8 (2016).

28. P. Pyykko, Atsumi M., Molecular single-bond covalent radii for elements 1-118, *Chemistry*, **15**, 1 (2009).